

Photodynamic parameters in the chick chorioallantoic membrane (CAM) bioassay for photosensitizers administered intraperitoneally (IP) into the chick embryo

Marie J. Hammer-Wilson,^{*a} Danielle Cao,^a Sol Kimel^{a,b} and Michael W. Berns^{*a}

^a Beckman Laser Institute, University of California, Irvine, CA 92612.

E-mail: mberns@bli.uci.edu; Fax: +1 949-824-8413; Tel: +1 949-824-6291

^b Department of Chemistry, Technion - Israel Institute of Technology, Haifa 32000, Israel

Received 6th June 2002, Accepted 7th June 2002

First published as an Advance Article on the web 16th July 2002

The chick chorioallantoic membrane (CAM) assay was used to determine the photodynamic response (PDR) of blood vessels to Photofrin[®], 5-aminolevulinic acid (ALA), benzoporphyrin derivative monoacid ring A (BPD-MA) and lutetium texaphyrin (Lutex). The photosensitizers were administered systemically *via* intraperitoneal injection into the chick embryo. Forward stepwise regression analysis of the PDR results enabled the individual contributions of seven experimental variables to be ranked: drug dose, light dose, fluence rate, drug uptake time, vessel type (whether arterioles or venules), vessel diameter, and embryo age. The order of importance of the variables, the PDR profile, was determined for each photosensitizer. Relative contributions of the experimental variables from this study to the CAM PDR were compared with those from our previous study on PDR of CAM blood vessels following topical application of the same photosensitizers. PDR profiles were interpreted in terms of biophysical and biochemical characteristics of the individual photosensitizers and the variation in their interactions with the delivery/distribution environment.

1 Introduction

With the advances of photodynamic therapy (PDT) of cancer¹ numerous second-generation photosensitizers (PS) are being considered to replace the standard Photofrin[®] II (PII).^{2,3} This creates a need for developing a model for the screening of photosensitizers that cover a wide range of photophysical and photochemical properties. The chick chorioallantoic membrane (CAM) has been previously used for testing of PS where vasculature was the primary target.⁴⁻⁸ The feasibility of using the CAM when implanted with tumors^{6,9} or other tissues¹⁰ for studying PS localization and to permit PDT evaluation¹¹ has been demonstrated. By combining these two uses of the CAM, it may be possible to develop a system for rapid screening of the efficacy of various PS in treating implanted tumors which would ultimately allow the creation of individualized patient treatment strategies. With this goal in mind, we have used the CAM to test four PS under several well-defined PDT conditions and examined whether the resulting photodynamic response (PDR) could be correlated with the parameters used.

2 Materials and methods

2.1 Photosensitizers (PS)

Stock solutions were prepared in accordance with the manufacturers' specifications.

Porfimer sodium (QLT, Vancouver, Canada), 20 mg ml⁻¹ in 5% dextrose; this preparation was considered to be equivalent to Photofrin[®] (PII).

5-Aminolevulinic acid – ALA (DUSA Pharmaceuticals, Inc., Denville, NJ), 25 mg ml⁻¹ in H₂O (adjusted to pH ≈ 6 with 10 N NaOH) was prepared freshly before each experiment.

Benzoporphyrin derivative mono acid – BPD-MA (QLT, Vancouver); the liposomal powder was reconstituted in H₂O, 2 mg ml⁻¹.

Lutetium texaphyrin – Lutex (Compound PCI-0123, Pharmacocyclics Inc., Sunnyvale, CA), 2 mg ml⁻¹ in 5% mannitol.

Photofrin[®] and Lutex were stored frozen at –20 °C in 1 ml aliquots and used once after thawing. BPD was stored at 4 °C for a maximum of three weeks. Working solutions of PII, ALA and Lutex were freshly prepared by dilution with the appropriate solvent. Final BPD solutions were prepared by dilution with 5% dextrose.

2.2 CAM preparation

The CAM as an *in vivo* bioassay for PDR has been described previously⁴⁻⁷ and was adopted here with minor modifications. Briefly, fertilized chicken eggs were disinfected and transferred to a tilting hatching incubator set at 38 °C and 60% humidity. At day 4 of embryo age (EA4), 4–5 ml albumin was aspirated with a 20 gauge needle, through a hole drilled at the narrow apex, to create a false air sac. At EA7, a 25 mm diameter window was cut into the shell and covered with a sterile Petri dish; incubation was continued in a static incubator.

2.3 Photosensitizer delivery

At EA12 or EA13, when the CAM had matured, 30 µl or 40 µl, respectively, of PS solution was injected into the chick embryo abdomen using a 30 gauge needle. Since in over 95% of the cases, injection did not cause embryo death, we infer that the PS was deposited in the intraperitoneal cavity and not in vital organs. The amounts administered were chosen to compensate for embryo growth, measured as 3.5 ± 0.3 g wet weight at EA12 and 4.7 ± 0.5 g at EA13, which represents the mean value of 30 embryos weighed at each age. A sterile Teflon O-ring (6 mm i.d., 1.4 mm annular width) was placed aseptically on a well-vascularized site of the CAM to define a 30 mm² region of interest. A sterile, blackened Petri dish was placed over the eggshell opening and all further manipulations were performed

in subdued light. Preliminary toxicity tests were done to determine the maximal non-lethal dose for each photosensitizer. None of the final doses selected exceeded 80% of the maximal non-lethal amount.

2.4 Irradiation parameters

Irradiation wavelengths were 630 nm (with PII), 635 nm (with ALA), 690 nm (with BPD) and 740 nm (with Lutex). CW radiation at 630 nm, 635 nm, and 690 nm was delivered by an argon-laser-pumped-dye laser, Model CR599 (Coherent, Palo Alto, CA) and at 740 nm by a stacked-diode laser (Lawrence Livermore Laboratories, Livermore, CA). The laser light was transmitted through a 400 μm multimode fiber, terminated with an uncoated microlens (PDT Systems, Santa Barbara, CA) which expanded the beam to cover the whole ring area ($\approx 60 \text{ mm}^2$, including the annular width). Laser output was determined using a Coherent Model 210 power meter. Eggs without PS were irradiated at each wavelength to determine at which light dose (fluence, J cm^{-2}) damage occurred. All irradiation conditions were well below these light doses. Fluence rates used were 33 mW cm^{-2} (with irradiation time 150 s or 300 s) or 100 mW cm^{-2} (with irradiation time 50 s or 100 s). With both fluence rates, the same total light doses (5 J cm^{-2} and 10 J cm^{-2}) were obtained.

2.5 Photodynamic response (PDR)

Preliminary experiments were carried out for each PS to determine the threshold drug dose causing vascular damage at the lower light dose (5 J cm^{-2}), and the maximal drug dose which when combined with the highest light dose (10 J cm^{-2}) did not routinely result in hemorrhage of the larger vessels. Groups of 5 eggs were treated as follows: controls (no drug, no light), dark toxicity (drug only), light sensitivity (irradiation only), and 48 experimental groups using a choice of treatment variables. These included: two light doses (5 J cm^{-2} and 10 J cm^{-2}) delivered at two time points (30 and 90 minutes after drug injection), two power densities (33 mW cm^{-2} and 100 mW cm^{-2}), three drug dosages and two embryo ages (EA12 and EA13). Thus, at least $2 \times 2 \times 2 \times 3 \times 2 \times 5 = 240$ eggs were used for each drug. After irradiation, eggs were covered with blackened Petri dishes and returned to the incubator.

2.6 Video microscopic documentation

Immediately prior to drug injection and also at one hour post-irradiation, the CAM area inside the O-ring was videotaped with a CCD color camera (Sony, model DXC-101) mounted on a stereomicroscope (Olympus, model SZH), using oblique illumination provided by a fiber optic light guide (Fiber Lite series 180, Dolan-Jenner Industries, Inc., Lawrence, MA). Final magnification at the TV monitor was $70\times$. Quantitation of the PDR, *i.e.* damage to the CAM microcirculation, was determined from analysis of the videotapes. The CAM model allows direct observation of blood flow, thus enabling differentiation between pre-capillary arterioles (where blood flows from large to smaller vessels) and post-capillary venules (flow from small to larger vessels). Analysis was done in a double blind fashion by two independent readers.

2.7 Damage assessment

Analysis of the video images allowed determination of several gradations in vascular PDR. Using our previously described classification system:⁷ "slight damage" (coagulation or vasoconstriction) was assigned a score of 1 or 1.2; "moderate damage" (coagulation + constriction, or angiostasis) a score of 1.6 or 2; "severe damage" (stasis + vasodilation, or hemorrhage) a score of 2.5 or 3. These cases are exemplified in our previously published work (Fig. 1).^{7,12} Damage was also graded according to vessel diameter (d). We assigned the following

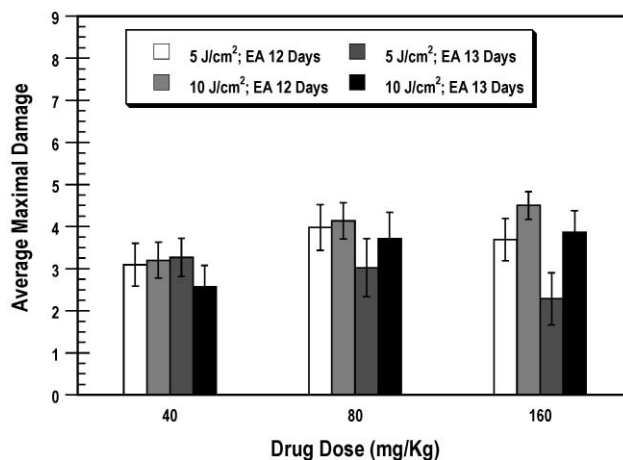


Fig. 1 Maximal damage scores for PII-based PDR in CAM blood vessels with light dose and embryo age as dominant treatment variables.

(arbitrary) weight factors to the damage score: 0, for "order-zero" capillaries ($d < 20 \mu\text{m}$); 1, for "order-1" venules or arterioles ($d \sim 40 \mu\text{m}$); 2, for "order-2" vessels ($d \sim 70 \mu\text{m}$); and 3, for "order-3" vessels ($d \sim 100 \mu\text{m}$). Typically, a CAM area inside a ring contained about seventy-five order-1 blood vessels, twenty-five order-2 vessels and ten order-3 vessels, with a slight preponderance of arterioles.¹³ For each egg, the weighted damage score was denoted as the highest value of the product (damage score) \times (vessel-order weight factor). Separate weighted damage scores were recorded for arterioles and venules. Drug doses were chosen such that hemorrhage of order-3 vessels, associated with score 9, was generally avoided.

2.8 Choice of treatment variables

In addition to the treatment variables commonly used in PDT, (a) drug type, (b) drug dose, (c) light dose, and (d) drug uptake time, we have added four treatment variables, in an effort to more fully elucidate the mechanism(s) of PDT. These are (e) fluence rate (less commonly studied in PDT), and three variables particularly suited to the CAM model: (f) vessel type (*i.e.*, arterioles and venules), (g) vessel diameter, and (h) embryo age (*i.e.*, embryonic development).

(a) The compounds used were three second-generation photosensitizers currently under active investigation¹⁻³ and the "standard" PII. They have different solubilities, span a wide range of photophysical and biochemical properties, and may localize in different subcellular targets.

(b) Three drug dosages were chosen which caused damage to the CAM vessels in the "linear region" of the dose response curve. The selected doses (in units of mg kg^{-1} wet embryo weight) were: PII 40, 80, 160; ALA 40, 80, 200; Lutex 4, 8, 16, and BPD 0.8, 2, 4.

(c) Light doses eliciting vascular PDR in the CAM model were lower⁵ than in other animal systems, because there are no losses due to absorption and scattering of radiation by overlying tissue. We have chosen 5 J cm^{-2} and 10 J cm^{-2} , which are about ten times lower than typical light doses used in animal and clinical PDT.

(d) A wide range of drug uptake times is used in PDT. One distinguishes between "fast" and "slow" acting PS, according to their characteristic half-lives ($t_{1/2}$) in plasma. For example, for PII $t_{1/2} = 8 \text{ h}$,¹⁴ for ALA $t_{1/2} = 1 \text{ h}$,¹⁴ for ALA's conversion product protoporphyrin IX (PpIX) $t_{1/2} = 1 \text{ h}$,¹⁴ for Lutex $t_{1/2} = 1.5 \text{ h}$,¹⁵ whereas for liposomally encapsulated BPD $t_{1/2} = 20 \text{ minutes}$.¹⁶ For all PS, the time course was monitored using uniform drug uptake times of 30 and 90 minutes prior to PDT. These times are probably too short for PII and too long for BPD. However, finding optimal uptake times was not our primary concern, since data are not directly transferable between different species such as avian embryos and rodents.

Instead, we concentrated on the dynamics associated with a threefold increase in uptake time.

(e) Fluence rates have reportedly been varied to study PDT-induced oxygen depletion,¹⁷ tissue response to PDT¹⁸ or hyperthermia effects.¹⁹ We have used two values (33 and 100 mW cm⁻²) and have kept the light dose constant by varying the irradiation time.

(f) Because of the difficulty in determining whether arterioles or venules constitute primary targets in vascular PDT, vessel type has been the subject of only few PDT studies; the main findings have been arteriole constriction and venule leakage.^{20,21} In the CAM, direct vessel visualization makes vessel type a practical parameter to examine.

(g) Vessel diameters in the CAM range from 20–120 μm,¹³ which encompasses typical diameters of neovasculature in tumors. Vessel diameters have been considered implicitly in the determination of weighted damage scores.

(h) The CAM model is characterized by a window of time for experimentation between EA10, when the CAM is complete, and EA17, when the embryo becomes immune competent. It is possible to perform PDT from EA10 onward. We have selected EA12 and EA13 to make results relevant for the tumor-bearing CAM model. In a variety of CAM tumor studies,^{6,22,23} tumor cells were implanted at EA8 and the eggs returned to the incubator until EA12 or EA13, when well-vascularized tumors were established of sufficient size for PDT treatment. The CAMs could then be monitored for an additional two to three days to determine PDT efficacy. It should be noted that the developing chick embryo and CAM is a dynamic system. Between EA12 and EA13 the embryo increases in weight by about 35% and extraembryonic tissue by about 15%.²⁴

2.9 Statistical analysis

For each PS, statistical analysis of damage scores was performed using a forward stepwise regression analysis to ascertain how well the treatment variables determine vascular damage. The first treatment variable entered into the regression equation is that with the strongest (positive or negative) correlation with vascular damage production. The absolute value of the standardized slope coefficient, β , expresses the strength of a parameter, while its sign (+/-) correlates with increase/decrease of PDR. The percent variance in vascular damage, which is accounted for by that treatment variable, is then calculated. The remaining treatment variables are added to the regression equation in successive steps. The stepwise regression algorithm selects the order of entry into the equation such that the treatment that adds the most additional explaining power to the existing regression is added next. For each PS, the “total percent of variance accounted for” by all variables is designated T-VAF. For each variable the percent of variance was normalized with respect to the T-VAF and is designated as “relative percent of variance accounted for” (R-VAF).

For the various conditions studied, the mean maximal damage \pm the standard error of the mean (SEM) was calculated. Where a parameter made only a minor contribution (< 0.1% of the T-VAF) to the damage it was collapsed into the other variables prior to calculating their means.

2.10 Topical application PS uptake

Photosensitizer solutions were prepared at the highest concentrations used in our previous topical application study.⁷ Tests were done using EA13 CAMs: 30 μl PS solution was placed in a ring (i.d. 6 mm) seated on the CAM surface and the egg returned to the incubator for 90 minutes. Following the uptake period, 20 μl of the PS was removed from the ring area and the absorption spectrum (at 1 : 100 dilution) was measured in a 2 ml cuvette with a Beckman DU650 spectrophotometer (Beckman Instruments, Fullerton, CA) using an optically matched blank. The difference between pre- and post-

incubation absorption at the major pre-incubation peak for each PS (see Table 5) was determined for a minimum of three samples, together with the mean and the SEM.

3 Results

In Table 1 we have collected the frequency of occurrence of maximal photodynamic response (PDR), differentiated according to vessel diameter (d). Maximal damage for a given d implies damage to vessels of smaller d . Thus for any damage score larger than 0, capillaries ($d < 40 \mu\text{m}$) are always damaged. Order-1 vessels ($d \sim 40 \mu\text{m}$) accounted for less than 0.1% of all maximal damage observations. In the majority of instances, an average of 76% over all photosensitizers (PS) examined, the maximum vascular damage sustained was equal for both vessel types. However, when the damage was not equal there was a marked tendency for arterioles to be more damaged. In order to compare the frequency of selective damage to the CAM arteries by the different PS, we have established a measure of vessel type response termed the arterial damage index (ADI). Since this damage response is also affected by vessel size, we have listed the values in Table 1. The arterial damage index was calculated by subtracting the cases where venules were more damaged than arterioles ($V > A$) from those where the inverse was true ($A > V$) and dividing by the total number of cases observed for all conditions: $\text{ADI} = [(A > V) - (V > A)] \div [(V > A) + (A > V) + (A = V)]$. ADI ranges from +1 to -1. A larger positive ADI corresponds to a higher fraction of arterioles *versus* venules sustaining maximal damage following treatment by the PS, whereas a larger negative ADI corresponds to a preponderance of damage to venules. The latter case ($\text{ADI} < 0$) has not been observed in this study.

Figs. 1–4 show the vascular PDR \pm SEM for the three most

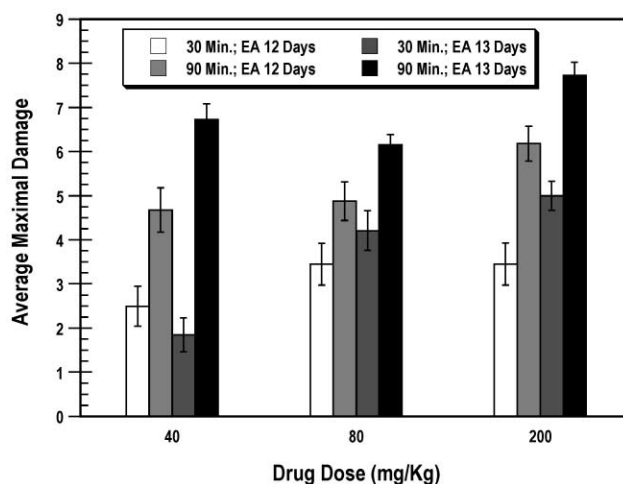


Fig. 2 Maximal damage scores for ALA-based PDR in CAM blood vessels with uptake time and embryo age as dominant treatment variables.

important treatment variables for each of the four PS used in this investigation. Ordinates represent mean maximal damage scores. Drug dose was utilized for the abscissa since it always ranked among the most important variables. Each group of four bars represents four parameter combinations; for each individual combination, $n = 20$.

Fig. 1 refers to PII for which the most important treatment variables, in addition to drug dose, were light dose (fluence, J cm⁻²) and embryonic age, EA (days). Correlation between the two independent, double-blinded readers was 0.86.

Fig. 2 refers to ALA where the predominant variables, along with drug dose, were uptake time (minutes) and EA. Reader correlation was 0.9.

Table 1 Frequency of maximal damage occurring in order-2 ($d \sim 70 \mu\text{m}$) and order-3 vessels ($d \sim 100 \mu\text{m}$), together with the preponderance of arterial damage exceeding venous damage

PS	Order-2 vessels		Order-3 vessels	
	Damage frequency	Arterial damage index	Damage frequency	Arterial damage index
PII	15%	0.42	85%	0.06
ALA	9%	0.30	91%	0.09
BPD	11%	0.15	89%	0.06
Lutex	19%	0.20	81%	0.06

Table 2 Relative percent of total damage to CAM blood vessels accounted for by the individual treatment variables for each photosensitizer (PS) following either intraperitoneal (IP) or topical administration. Treatment variables retained in Figs. 1–4 to explain photodynamic response following IP administration of PS are given in bold face

PS	Drug dose	Light dose	Fluence rate	Uptake time	EA
PII IP	15	22	5	12	46
PII topical	5	44	21	30	0
ALA IP	17	3	0	68	12
ALA topical	8	9	5	78	0
BPD IP	27	62	11	0	0
BPD topical	11	84	1	4	0
Lutex IP	61	27	1	10	1
Lutex topical	22	3	74	1	0

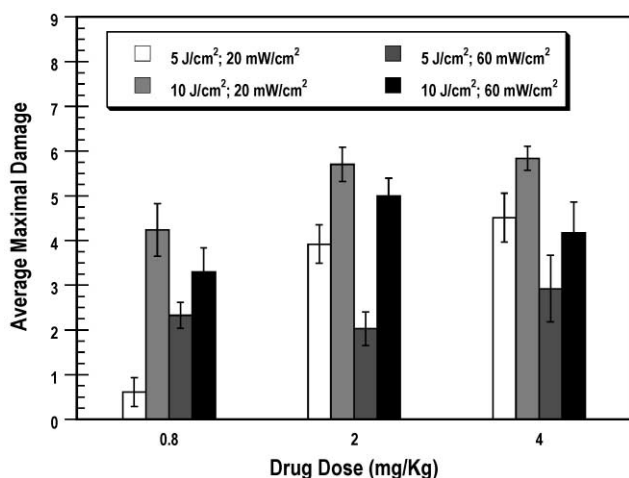


Fig. 3 Maximal damage scores for BPD-based PDR in CAM blood vessels with light dose and fluence rate as dominant treatment variables.

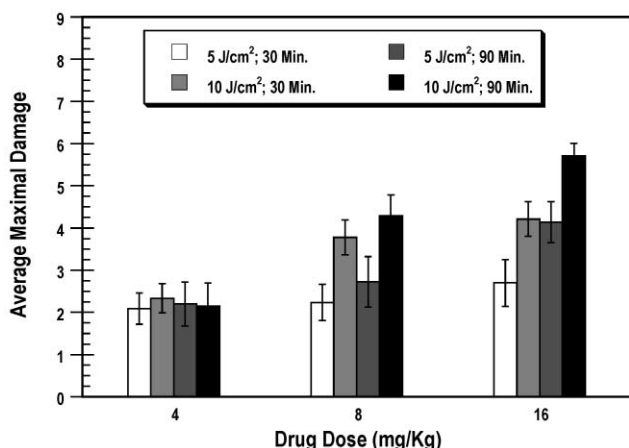


Fig. 4 Maximal damage scores for Lutetex-based PDR in CAM blood vessels with light dose and uptake time as dominant treatment variables.

Fig. 3 is for BPD where light dose and fluence rate (mW cm^{-2}) were the two most important variables besides drug dose. Reader correlation was 0.86.

Table 3 Total percent of damage to CAM blood vessels accounted for, from stepwise regression, by all five treatment variables for intraperitoneal (IP) and topical administration for each photosensitizer (PS)

PS	PII	ALA	BPD	Lutex
IP	4.1	43.2	23.8	18.9
Topical	16.9	27.4	11.1	53.8

Fig. 4 displays results for Lutetex for the variables light dose and uptake time, which followed drug dose in importance. Reader correlation was 0.79.

The choice of treatment variables used in Figs. 1–4 arises from the regression analysis presented in Table 2, in which the relative importance of individual parameters to account for damage (R-VAF) was tested. The three predominant ones are indicated in bold face. R-VAF entries are presented after normalization with respect to the total percent of damage accounted for (T-VAF), as given in Table 3. For comparative purposes, information on vascular damage following topical application of PS in the same bioassay⁷ is also included in Tables 2 and 3. Table 4 lists the β coefficients of all PS for the five treatment variables. In Table 5 we have quantified the amount of PS actually taken up across the chorion ectoderm during topical delivery. Initial and residual PS concentrations were determined from the absorption spectra taken after 0 and 90 minutes uptake time. Table 6 gives the comparative results of the drug doses needed to achieve a PDR in CAM vessels following either topical or IP delivery of the PS.

4 Discussion

The ideal system for testing PDT efficacy of PS on patient tumors should possess three characteristics: 1) the ability to grow the tumor cells in a “normal” 3D architecture complete with appropriate vasculature, 2) the possibility of testing the PS by multiple modes of delivery under otherwise identical conditions, and 3) ease of analysis of PDT effects. The CAM/chick embryo system would appear to possess all of these attributes. Tumors can be easily grown on it.^{6,9} Photosensitizers can be delivered topically,^{4,5,7,9,11} intravenously^{8,9} or intraperitoneally.⁶ The tumors can be excised from the CAM and histologically

Table 4 Standardized slope coefficients, β , for vascular damage accounted for by individual treatment variables following intraperitoneal administration of photosensitizer

	PS	Drug dose	Light dose	Fluence rate	Uptake time	EA
	PII	0.079	0.094	-0.042	0.070	-0.138
	ALA	0.271	0.118	0.003	0.544	0.221
	BPD	0.254	0.383	-0.163	0.011	0.011
	Lutex	0.342	0.229	-0.032	0.138	-0.031

Table 5 Uptake of photosensitizer (PS) through the CAM based on measured absorbance (A) of initial and residual topically applied solutions. Solutions (concentration C) were applied for 90 minutes to EA 13 CAMs

PS	$\lambda_{\text{peak}}/\text{nm}$	$C(t=0)/\mu\text{g ml}^{-1}$	$A(t=0)$	$C(t=90)/\mu\text{g ml}^{-1}$	$A(t=90)$	Uptake (%)
PII	284	0.5	0.043 ± 0.002	0.08	0.007 ± 0.001	84
ALA	264 ± 2	500	0.035 ± 0.001	460	0.032 ± 0.004	8
BPD	281	0.05	0.039 ± 0.002	0	0	100
Lutex	473 ± 2	2.5	0.087 ± 0.002	0.25	0.008 ± 0.002	90

Table 6 Comparison of photosensitizer (PS) dosages used for topical and intraperitoneal (IP) administration that result in photodynamic response in EA13 CAMs after 90 minutes of PS uptake

PS	Topical dose/ $\mu\text{g cm}^{-2}$	$D_{\text{top}} \mu\text{g}/\text{ring area}$	IP dose mg/kg	$D_{\text{IP}} \text{ng}/\text{ring area}$	$D_{\text{IP}}/D_{\text{top}}$
PII	1-5	0.25-1.25	40-160	600-2400	2.4
ALA	1000-5000	24-120	40-200	600-3000	0.025
BPD	0.1-0.5	0.03-0.15	0.8-4	12-60	0.4
Lutex	5-25	1.35-6.75	4-16	60-240	0.044

examined for tumor cell necrosis/apoptosis and vascular destruction.

Previously we reported on the PDR of the CAM vasculature when various PS were delivered topically.⁷ In this study we have examined the PDR of the CAM vasculature following IP delivery of four of the same PS. We have also compared the PDR profiles (the order of importance of the treatment variables) for these PS when delivered by the two application methods and discuss possible explanations for the profile differences.

Fig. 5 illustrates the differences between topical (external) and

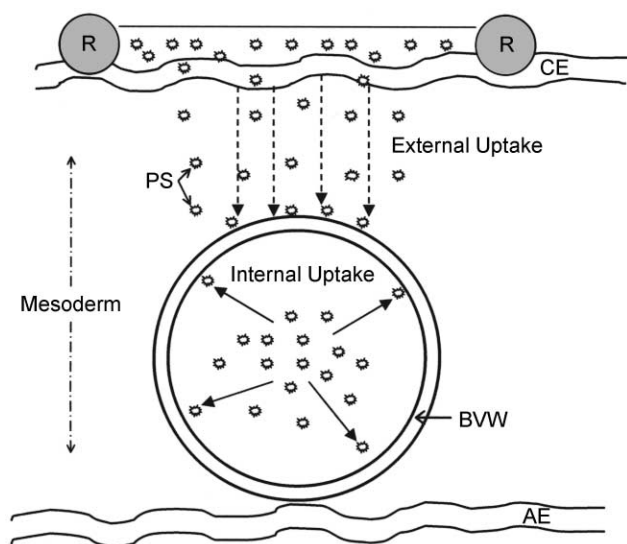


Fig. 5 Schematic representation of a cross-section through the ring area on the CAM and one underlying blood vessel (not to scale) showing PS uptake routes. R-ring; CE-chorion ectoderm; BVW-blood vessel wall; AE-allantoic endoderm; PS-photosensitizer.

IP (internal) administration. The amount of PS estimated to reach the vasculature in the ring area examined for each method of delivery is presented in Table 6.

Topical: PS diffuses locally across the intact external membrane layer (the chorion ectoderm) of the CAM,

percolates through the mesoderm, and is taken up in part by endothelial cells of blood vessels present therein. This is termed “external” uptake (Fig. 5). Applied dosages ranged from 0.1–25 $\mu\text{g cm}^{-2}$, with the exception of ALA for which dosages ranged from 1000–5000 $\mu\text{g cm}^{-2}$ (Table 6, column 2). Actual amounts of PS that crossed the chorion ectoderm of the EA13 CAM (Table 5, column 7) were factored in when calculating D_{top} ($\mu\text{g}/\text{ring area}$).

IP: The PS dose at EA13 in the CAM area demarcated by the ring, D_{IP} (Table 6, column 5), was calculated by taking the amount of PS per embryo {the PS concentration (mg ml^{-1}) \times the amount injected ($40 \mu\text{l}$) \times the embryo wet weight (4.8g)} \times the percentage of the embryo blood present in the CAM and multiplying that value by the percent of the CAM enclosed by the ring. It was assumed that the entire dose of PS was taken up into the embryo’s blood of which 60% is present in the mature CAM.²⁴ The ring area (30mm^2) constitutes 0.5% of the total CAM area ($\sim 6000 \text{mm}^2$). From blood circulating through the extra-embryonic vasculature, endothelial cells take up PS by a process termed “internal” uptake (Fig. 5). The ratios ($D_{\text{IP}}/D_{\text{top}}$) are listed in the last column of Table 6. For all PS except PII, D_{top} (column 3) is larger than D_{IP} (column 5) but the ratios obtained are difficult to interpret. For example, the 50-fold difference between the values for Lutex and PII may be related in some way to their hydrophilic/phobic nature, but a more precise understanding must await further experimentation.

Based on the comparisons in Table 6, it would appear that systemic delivery (IP) is a more efficient method of delivering ALA, BPD and Lutex than topical application. Efficiency of delivery, however, is not the same as efficacy of PDR. If the two were positively correlated, consistently more damage would be accounted for when using IP delivery and the order of influence of the parameters explored would be unchanged for each PS. Clearly this is not the case. Table 2 reveals that the pattern of parameter contributions to PDR is changed when the delivery method is changed. For PII the high $D_{\text{IP}}/D_{\text{top}}$ ratio in Table 6 and the low percent of damage accounted for with IP delivery (Table 3) suggests that some additional factor must be influencing the damage produced using IP delivery of the PS.

The most obvious difference between topical and IP delivery of PS, is the environment that the PS experiences as it makes its way from the point of administration to the target endothelial

cells, (see Fig. 5). The composition of the CAM is essentially static, both structurally and chemically, from day 10 through day 17.^{13,24} The topically applied PS traverses a thin ectodermal membrane and then passes through the mesoderm, which is sparsely populated with fibroblasts, to the endothelial cells. Here the PS passes essentially through a homogenous medium where there is little diffusion and mixing with other components. On the other hand, IP administered PS is taken up into the circulatory system of the embryo. There it experiences an environment where other solutes interact with it. The PS is exposed to many different cell types, which may bring about chemical alterations, and it is continually mixed with other blood components. Additionally, the chemical environment is changing as the serum components change with embryo age.²⁴ Moreover, the composition of serum in the chick embryo is different from that found in mice, which are commonly used to test PS for PDT efficacy, and in humans. On EA12 and EA13 chick embryo serum contains approximately 95% water, with only about 12 mg ml⁻¹ protein and about 2.5 mg ml⁻¹ lipoprotein. Mammalian serum (mouse and human) contains between 65–75% water, with 55–70 mg ml⁻¹ protein and 15–20 mg ml⁻¹ lipoprotein.^{25,26} For humans, low density lipoprotein is predominant, while for mouse and chick embryo it is primarily high density lipoprotein (HDL).^{25–27} Uptake and distribution of porphyrin-type PS are strongly influenced by the lipid composition of the carrier, *i.e.* serum, in IP delivery.^{1,25,26} Another significant difference between mammalian and avian blood is the presence of nuclei in avian erythrocytes.²⁴

We now discuss PDR for each of the PS tested in terms of their T-VAF given in Table 3, the R-VAF values for the PDR parameters examined in Table 2, and the influence of the delivery environment.

PII

For IP administration, the lack of influence of all treatment variables (T-VAF = 4.1%) may be understood in view of the efficient binding of PII to the HDL of chick embryo serum. This will lead to minimal change in PDR when varying drug dose since in embryos the bulk of PII is unavailable for transfer to the endothelial cells. This should be contrasted with drug-dose response of PII in other animal systems (or in clinical studies) where the fast growing tumor represents but a small weight fraction of the whole animal. Also, uptake of PII has been shown to be larger when the serum contains a high proportion of very low density lipoprotein,²⁵ which is not the case for chick embryo serum.²⁷ EA influences the serum composition²⁴ and accounts for nearly 50% of the T-VAF. The negative value of the β coefficient for EA ($\beta = -0.138$) implies less PII is available for PDR which correlates with the presence of more HDL to bind PII with increasing embryo development.^{24,27} Moreover, the PII dose required for measurable PDR was out of range compared to accepted clinical drug doses, and in fact was close to the lethal dose. The three remaining treatment variables contributed even less than EA and in view of the low T-VAF were not considered significant. For topical application, T-VAF was substantially greater (16.9%) than for IP administration (4.1%). Most probably this is because target sites are reached without interaction with the embryo's serum. Consequently, EA now does not contribute to PDR at all (R-VAF = 0). Retention of the PII that is incorporated into the endothelial cells is enhanced by the low protein, high water content of chick embryo serum which prevents efficient PS clearance²⁵ resulting in the uptake time becoming more important (R-VAF = 30%). With more PS present, light dose increases in importance (R-VAF = 44%).

ALA

It is well known that ALA requires intracellular conversion to PpIX before becoming photoreactive. Reported PpIX concen-

trations following intravenous²⁸ or IP²⁹ administration of ALA indicate conversion efficiencies less than 1% in healthy tissues. Consequently, for IP administered ALA uptake time is the dominant treatment variable (R-VAF = 68% with a large positive coefficient, $\beta = 0.544$). With IP delivery the entire embryo, including the red blood cells, participates in the conversion of ALA to PpIX, which is then transported throughout the CAM. Correspondingly, the amount of the precursor ALA available for conversion is also important (R-VAF = 17% with positive correlation, $\beta = 0.271$). Embryo age is a contributing factor (R-VAF = 12% with $\beta = 0.221$) due to increased metabolic competence as the embryo matures. Because ALA is hydrophilic and does not bind to any serum components,¹⁴ the chemical composition of embryo serum does not affect its delivery to the vessel endothelium. For topical application, T-VAF was smaller (27.4%) than that for IP administration (43.2%). Most likely this is due to the conversion of the externally applied ALA to PpIX being confined to the immediately adjacent CAM vessels. As with IP delivery, uptake time is the most important factor (R-VAF = 78%) for topical application. Embryo age is not important (R-VAF = 0) since the CAM is already functionally mature by day 10. The effect of drug dose is reduced (R-VAF = 8%) since the number of endothelial cells in the ring area is limited and the amount of ALA delivered probably exceeds their conversion capacity. With the amount of PpIX essentially fixed by the number of endothelial cells present, the light dose (R-VAF = 9%) and fluence rate (R-VAF = 5%) begin to influence the PDR outcome.

BPD

Since BPD is encapsulated in liposomes, consisting of about 80 times more dimyristoyl phosphatidyl choline than BPD,³⁰ "internal" uptake by endothelial cells was immediate (R-VAF = 0 for uptake time). Being contained by its own lipid carrier, the composition of embryo serum does not influence PS uptake. However, the influence of drug dose was limited by the cellular capacity to incorporate the liposomal material (R-VAF = 27%). Consequently, light dose takes on added significance (R-VAF = 62%) probably because of the reciprocal drug and light dose relationship for achieving a given PDR. As a corollary, the fluence rate also becomes important (R-VAF = 11%) because of oxygen depletion at the higher photon flux (as corroborated by the negative coefficient $\beta = -0.163$). The smaller T-VAF for the topically applied drug (11.1%) *versus* that delivered systemically (23.8%) is probably due to more effective delivery of intact liposomes to the target cells by circulating blood. The lower drug dose response for topical application (R-VAF = 11%) *versus* that for IP (R-VAF = 27%) would also support the possibility that the quantity of encapsulated BPD able to cross the chorion ectoderm is limited by the capacity of the ring area to absorb the outer lipid layers of the transiting liposomes, thus restricting the final amount of BPD available for cellular incorporation. With lower drug dose contribution to PDR for topically applied BPD, the light dose importance increases to an even greater level (R-VAF = 84%) than seen with IP delivery.

Lutex

Like PII, this porphyrin derived compound is affected by the lipoprotein environment in which it is delivered.²⁶ Its probable affinity for the HDL fraction of the embryo serum is the most likely explanation for the relatively low overall T-VAF (18.9%) seen with IP delivery. Uptake of this water soluble compound follows diffusion driven uptake kinetics with drug concentration the most influential parameter (drug dose R-VAF = 61%). The high R-VAF for drug dose was accompanied by a low one for light dose (27%), again reflecting the inverse relationship between the two parameters as seen with other PS. For topical application the high T-VAF (53.8%) and low contribution of uptake time (R-VAF = 1%) is consistent with a compound that

easily passes through membranes and requires no alteration to render it effective. Like PII, once the compound has entered the endothelial cells its retention is probably enhanced by chick embryo serum composition preventing its washout. The unusual influence of the fluence rate (R-VAF = 74%) is unexplained at this time, but has also been observed in treatment of murine SMTF tumors.³¹

The preponderance of arterial damage compared to venous damage (Table 1) seems to be a general phenomenon, observed in the CAM both for PDR⁷ and photothermolysis.^{12,32} It is probably due to hemodynamics since photo-induced thrombi cause downstream obstruction in the arteriolar network. It should be noted that PDT in the vasculature of rodents also causes preferential arterial damage²¹ so that the phenomenon is not due to the fact that in the CAM arterioles transport deoxygenated blood.

5 Conclusions

PII

Since the PDT efficacy of PII is influenced by its delivery environment, the disparity between chick embryo and mammalian serum composition makes it unlikely that the CAM system can be used to reliably predict drug-tumor interactions in humans when using systemic delivery. Thus, the CAM assay is probably not suitable for testing IP administered PII with implanted tumors. In contrast, topically applied PII is less likely to be influenced by the delivery environment and could be used to test for tumor response to the drug. The T-VAF values of 4.1% versus 16.9% for IP and topical application support this conclusion. Additionally, the large impact of EA on the PDR of IP delivered PII would argue against using this model except with strictly controlled EA conditions.

ALA

The relatively large T-VAF values for both IP (43.2%) and topical (27.4%) administration suggest that the CAM system may be satisfactory for screening PDR of ALA in implanted tumors using both delivery methods. Since ALA is a naturally occurring compound used for heme production in chickens as well as mammals, it is not surprising that it appears to work well.

BPD

Despite the moderate T-VAF value for IP administration (23%), the ability of interpreting the relationship between the 2 primary treatment variables (drug and light dose) makes the CAM system reasonable to consider for screening PDR with BPD. For topical application, the CAM system appears less suitable since BPD is released locally following fusion of the liposomal carrier with the chorion ectoderm. However, this may prove not to be a problem with implanted tumors, when the liposomes could fuse directly with tumor cells growing through the chorion, thus eliminating the concern of not enough encapsulated drug reaching the target tissue.

Lutex

The low T-VAF value obtained in the present study (18.9%) should be contrasted with the high value for topical application (53.8%), making the CAM system less attractive for screening purposes when using IP administration of this PS.

In the CAM system, systemically delivered photosensitizers do not behave the same as their topically applied counterparts. For each PS there is an application method that appears superior in terms of explaining the observed PDR. Also, for each PS the relative importance of the PDT parameters examined changes with the method of delivery. This would seem to

preclude developing a "universal" CAM-based screening methodology allowing direct comparison of different PS. Instead, the CAM assay may be best suited for testing individual photosensitizers for their ability to induce a PDT response, provided the chemical nature of the PS is taken into account when choosing the test conditions.

Acknowledgements

The authors thank Marianne Bergheim and Christine Torralba for technical assistance and Jeff Andrews for help with the laser set-ups. Dr Anita L. Iannucci, UCI Center for Statistical Consulting, performed the statistical analysis. Institutional support from the AFOSR (F49620-00-1-0371), the ONR (N00014-94-1-0874), the DOE (DE-FG03-91ER61227), the NIH (5RO1 CA 32248-14 and RR-01192) and the Beckman Laser Institute Endowment is gratefully acknowledged.

References

- 1 T. J. Dougherty, C. J. Gomer, B. W. Henderson, G. Jori, D. Kessel, M. Korbelik, J. Moan and Q. Peng, Photodynamic therapy, *J. Natl. Cancer Inst.*, 1998, **90**, 889–905.
- 2 R. W. Boyle and D. Dolphin, Structure and biodistribution relationships of photodynamic sensitizers, *Photochem. Photobiol.*, 1996, **64**, 469–485.
- 3 G. Jori, Tumour photosensitizers: Approaches to enhance the selectivity and efficiency of photodynamic therapy, *J. Photochem. Photobiol. B*, 1996, **36**, 87–93.
- 4 V. Gottfried, E. S. Lindenbaum and S. Kimel, Vascular damage during PDT as monitored in the chick chorioallantoic membrane, *Int. J. Radiat. Biol.*, 1991, **60**, 349–354.
- 5 V. Gottfried, R. Davidi, C. Averbuj and S. Kimel, In vivo damage to chorioallantoic membrane blood vessels by porphycene-induced photodynamic therapy, *J. Photochem. Photobiol. B*, 1995, **30**, 115–121.
- 6 R. Hornung, M. J. Hammer-Wilson, S. Kimel, L. H. Liaw, Y. Tadir and M. W. Berns, Systemic application of photosensitizers in the chick chorioallantoic membrane (CAM) model: photodynamic response of CAM vessels and ALA uptake kinetics by transplantable tumors, *J. Photochem. Photobiol. B*, 1999, **49**, 41–49.
- 7 M. J. Hammer-Wilson, L. Akian, J. Espinoza, S. Kimel and M. W. Berns, Photodynamic parameters in the chick chorioallantoic membrane (CAM) bioassay for topically applied photosensitizers, *J. Photochem. Photobiol. B*, 1999, **53**, 44–52.
- 8 N. Lange, J. P. Ballini, G. Wagnieres and H. van den Bergh, A new drug-screening procedure for photosensitizing agents used in photodynamic therapy for CNV, *Invest. Ophthalmol. Vis. Sci.*, 2001, **42**, 38–46.
- 9 A. Rück, N. Akgün, K. Heckelsmiller, G. Beck, F. Genze and R. Steiner, Confocal observation of hydrophilic and lipophilic photosensitizers in endothelial cells, lumen of the vessels, interstitium and tumor cells using the chicken chorioallantoic membrane, *Proc. SPIE-Int. Soc. Opt. Eng.*, 1998, **3247**, 63–68.
- 10 K. Kunzi-Rapp, A. Rück and R. Kaufmann, Characterization of the chick chorioallantoic membrane model as a short-term in vivo system for human skin, *Arch. Dermatol. Res.*, 1999, **291**, 290–295.
- 11 M. S. Ismael, U. Torsten, C. Dressler, J. E. Diederichs, S. Hueske, H. Weitzel and H. P. Berlien, Photodynamic therapy of malignant ovarian tumours cultivated on CAM, *Lasers Med. Sci.*, 1999, **14**, 91–96.
- 12 S. Kimel, L. O. Svaasand, D. Cao, M. J. Hammer-Wilson and J. S. Nelson, Vascular response to laser photothermolysis as a function of pulse duration, vessel type and diameter: implications for port wine stain laser therapy, *Lasers Surg. Med.*, 2002, **30**, 160–169.
- 13 D. O. DeFouw, V. J. Rizzo, R. Steinfeld and R. N. Feinberg, Mapping of the microcirculation in the chick chorioallantoic membrane during normal angiogenesis, *Microvasc. Res.*, 1989, **38**, 333–336.
- 14 Q. Peng, T. Warloe, K. Berg, J. Moan, M. Kongshaug, K. E. Giercksky and J. M. Nesland, 5-Aminolevulinic acid-based photodynamic therapy. Clinical research and future challenges, *Cancer*, 1997, **79**, 2282–2308.
- 15 S. W. Young, K. W. Woodburn, M. Wright, T. D. Mody, Q. Fan, J. L. Sessler, W. C. Dow and R. A. Miller, Lutetium texaphyrin (PCI-0123): a near-infrared, water-soluble photosensitizer, *Photochem. Photobiol.*, 1996, **63**, 892–897.

- 16 A. M. Richter, E. Waterfield, A. K. Jain, B. Allison, E. D. Sternberg, D. Dolphin and J. G. Levy, Photosensitizing potency of structural analogues of benzoporphyrin derivative (BPD) in a mouse tumor model, *Br. J. Cancer*, 1991, **63**, 87–93.
- 17 R. Sorensen, V. Iani and J. Moan, Kinetics of photobleaching of protoporphyrin IX in the skin of nude mice exposed to different fluence rates of red light, *Photochem. Photobiol.*, 1998, **68**, 835–840.
- 18 T. M. Sitnik and B. W. Henderson, The effect of fluence rate on tumor and normal tissue responses to photodynamic therapy, *Photochem. Photobiol.*, 1998, **67**, 462–466.
- 19 S. Kimel, L. O. Svaasand, M. Hammer-Wilson, V. Gottfried, S. Cheng, E. Svaasand and M. W. Berns, Demonstration of synergistic effects of hyperthermia and photodynamic therapy using the chick chorioallantoic membrane model, *Lasers Surg. Med.*, 1992, **12**, 432–440.
- 20 A. Major, S. Kimel, S. Mee, T. E. Milner, D. J. Smithies, S. M. Srinivas, Z. Chen and J. S. Nelson, Microvascular photodynamic effects determined *in vivo* using optical Doppler tomography, *IEEE J. Sel. Top. Quantum Electron.*, 1999, **5**, 1168–1175.
- 21 V. H. Fingar, T. J. Wieman, S. A. Wiehle and P. B. Cerrito, The role of microvascular damage in photodynamic therapy: the effect of treatment on vessel constriction, permeability, and leukocyte adhesion, *Cancer Res.*, 1992, **52**, 4914–4921.
- 22 M. Nguyen, Y. Shing and J. Folkman, Quantitation of angiogenesis and antiangiogenesis in the chick embryo chorioallantoic membrane, *Microvas. Res.*, 1994, **47**, 31–40.
- 23 D. Ribatti, A. Vacca, L. Roncali and F. Dammacco, The chick embryo chorioallantoic membrane as a model for *in vivo* research on anti-angiogenesis, *Curr. Pharm. Biotechnol.*, 2000, **1**, 73–82.
- 24 A. L. Romanoff, A. J. Romanoff, *Biochemistry of avian embryo: a quantitative analysis of prenatal development*, Interscience Publishers, New York, 1967.
- 25 M. Korbelik, Cellular delivery and retention of Photofrin: II. The effects of human *versus* mouse and bovine serum, *Photochem. Photobiol.*, 1992, **56**, 391–397.
- 26 K. W. Woodburn, Q. Fan, D. Kessel, Y. Luo and S. W. Young, Photodynamic therapy of B16F10 murine melanoma with lutetium texaphyrin, *J. Invest. Dermatol.*, 1998, **110**, 746–751.
- 27 M. Kanai, T. Soji, E. Sugawara, N. Watari, H. Oguchi, M. Matsubara and D. C. Herbert, Participation of endodermal epithelial cells on the synthesis of plasma LDL and HDL in the chick yolk sac, *Microscopy Res. Tech.*, 1996, **35**, 340–348.
- 28 C. S. Loh, D. Vernon, A. J. MacRobert, J. Bedwell, S. G. Bown and S. B. Brown, Endogenous porphyrin distribution induced by 5-aminolaevulinic acid in the tissue layers of the gastrointestinal tract, *J. Photochem. Photobiol. B*, 1993, **20**, 47–54.
- 29 B. W. Henderson, L. Vaughan, D. A. Bellnier, H. van Leengoed, P. G. Johnson and A. R. Oseroff, Photosensitization of murine tumor, vasculature, and skin by using 5-aminolevulinic acid-induced porphyrin, *Photochem. Photobiol.*, 1995, **62**, 780–789.
- 30 A. M. Richter, E. Waterfield, A. K. Jain, A. J. Canaan, B. A. Allison and J. G. Levy, Liposomal delivery of photosensitizer, benzoporphyrin derivative monoacid ring (BPD) to tumor tissue in a mouse tumor model, *Photochem. Photobiol.*, 1993, **57**, 1000–1006.
- 31 M. J. Hammer-Wilson, personal communication, 1999.
- 32 S. Kimel, L. O. Svaasand, M. Hammer-Wilson, M. J. Schell, T. E. Milner, J. S. Nelson and M. W. Berns, Differential vascular response to laser photothermolysis, *J. Invest. Dermatol.*, 1994, **103**, 693–700.